New Phytologist

Research

Synchrotron X-ray microtomography of xylem embolism in *Sequoia sempervirens* saplings during cycles of drought and recovery

Brendan Choat[1], Craig R. Brodersen[2] and Andrew J. McElrone[3,4]

[1]Hawkesbury Institute for the Environment, University of Western Sydney, Richmond, NSW 2753, Australia; [2]School of Forestry & Environmental Studies, Yale University, 195 Prospect Street, New Haven, CT 06511, USA; [3]USDA-Agricultural Research Service, Davis, CA 95616, USA; [4]Department of Viticulture and Enology, University of California, Davis, CA 95616, USA

Author for correspondence:
Brendan Choat
Tel: +61 2 4570 1901
Email: b.choat@uws.edu.au

Received: *11 July 2014*
Accepted: *10 September 2014*

New Phytologist (2014)
doi: 10.1111/nph.13110

Key words: cavitation, embolism, microCT, redwood, refilling, *Sequoia*, xylem.

Summary

- The formation of emboli in xylem conduits can dramatically reduce hydraulic capacity and represents one of the principal mechanisms of drought-induced mortality in woody plants. However, our understanding of embolism formation and repair is constrained by a lack of tools to directly and nondestructively measure these processes at high spatial resolution.
- Using synchrotron-based microcomputed tomography (microCT), we examined embolism in the xylem of coast redwood (*Sequoia sempervirens*) saplings that were subjected to cycles of drought and rewatering.
- Embolism formation was observed occurring by three different mechanisms: as tracheids embolizing in wide tangential bands; as isolated tracheids in seemingly random events; and as functional groups connected to photosynthetic organs. Upon rewatering, stem water potential recovered to predrought stress levels within 24 h; however, no evidence of embolism repair was observed even after a further 2 wk under well-watered conditions.
- The results indicate that intertracheid air seeding is the primary mechanism by which embolism spreads in the xylem of *S. sempervirens*, but also show that a small number of tracheids initially become gas-filled via another mechanism. The inability of *S. sempervirens* saplings to reverse drought-induced embolism is likely to have important ecological impacts on this species.

Introduction

In order to extract water from the soil and transport it to the canopy, plants utilize a unique transport mechanism in which liquid water is held under tension (Dixon & Joly, 1895; Tyree & Zimmermann, 2002). In this state, water is considered to be under negative pressure and therefore metastable. Although there was initial scepticism over the existence of 'stretched water', there is now overwhelming evidence that under suitable conditions, water can remain in the liquid phase at many MPa below absolute zero pressure (Briggs, 1950; Oertli, 1971; Zheng *et al.*, 1991; Debenedetti, 2013). The existence of liquid water under tension has also been confirmed in plants by pressure probe measurements made directly on xylem vessels of transpiring plants (Melcher *et al.*, 1998; Wei *et al.*, 1999). More recently, water transport under tension was simulated in a 'synthetic tree' constructed of polymer microchannel networks (Wheeler & Stroock, 2008).

One consequence of water being held in a metastable state is the risk of the xylem sap rapidly changing from the liquid phase to the vapour phase. This process, known as cavitation, produces an audible 'click' as energy is released from the hydrogen bonds holding the water together as a liquid (Milburn, 1973). The resulting gas embolism becomes trapped in the xylem conduit, thereby blocking water transport and reducing the total hydraulic capacity of the plant. This is particularly problematic during droughts because lower water potential in the soil and high evaporative demand at the leaf–air interface cause tension in the xylem sap to increase, thus increasing the probability of cavitation. In order to maintain xylem water potentials above the crucial pressures that cause significant cavitation in the stem, plants must close their stomata, leading to rapid declines in photosynthesis (Martorell *et al.*, 2014). In severe droughts, xylem embolism may result in the death of whole plants (Brodribb & Cochard, 2009; Choat, 2013; Urli *et al.*, 2013), and drought-induced embolism is now recognized as one of the key traits controlling drought-induced mortality in woody plants (Choat *et al.*, 2012).

Drought-induced cavitation is thought to occur via air seeding, the movement of gas through pit membranes between adjacent xylem conduits (Zimmermann & Brown, 1971; Tyree & Sperry, 1989). As the pressure difference between gas-filled and water-filled conduits increases, the probability of gas being pulled through the pit membranes increases (Choat *et al.*, 2008;

Pittermann *et al.*, 2010). This mechanism of cavitation is far more likely than homogeneous nucleation in the bulk phase, based on both theoretical grounds and indirect experimental evidence (Pickard, 1981; Pockman *et al.*, 1995). Air seeding between xylem vessels has also recently been visualized directly in an angiosperm species by synchrotron-based microcomputed tomography (microCT) (Brodersen *et al.*, 2013a). However, angiosperm and gymnosperm pit membrane structure and function differ considerably (Pittermann *et al.*, 2005; Choat & Pittermann, 2009). In angiosperms, nanoscale pores in the pit membranes prevent air seeding until a critical pressure difference is reached, allowing air to be aspirated from a vapour-filled conduit to a water-filled conduit across the shared wall and pit membrane (Sperry & Tyree, 1988; Choat *et al.*, 2004). In the majority of gymnosperms, a thickened torus in the centre of the pit membrane serves to plug the pit aperture and prevent the spread of cavitation to adjacent tracheids (Bailey, 1913). At some critical pressure, air seeding occurs via pores in the torus or because the torus slips from the pit aperture (Sperry & Tyree, 1990; Hacke *et al.*, 2004; Domec *et al.*, 2006; Delzon *et al.*, 2010; Pittermann *et al.*, 2010; Jansen *et al.*, 2012). However, the dynamics of embolism spread in species with tracheid-based xylem has not been documented in detail.

Although the effects of embolism can be disastrous for plants, some species can recover their hydraulic capacity by dissolving gas emboli and restoring xylem conduits to a functional, liquid-filled state. When examining mechanisms of embolism repair, it is necessary to differentiate between seasonal refilling and rapid refilling that takes place on hourly timescales after water stress-induced embolism formation. The former is a well-documented process by which many temperate tree and vine species recover conductive capacity in the spring after suffering freeze-induced embolism in winter. This is usually achieved by means of positive pressure generated in the roots or stems (Sperry *et al.*, 1987; Ameglio *et al.*, 2001; Cobb *et al.*, 2007). The thermodynamics of this refilling process are relatively straightforward, because the bulk xylem water potential is positive, allowing gas to be dissolved back into solution or forcing it from the stem.

Observations of rapid refilling of xylem conduits are more puzzling. A number of studies indicate that refilling occurs during daylight hours, with some suggesting that refilling takes place when xylem is under tension (Salleo *et al.*, 1996; McCully, 1999; Holbrook & Zwieniecki, 1999; Tyree *et al.*, 1999; Stiller *et al.*, 2005; Brodersen *et al.*, 2010; Martorell *et al.*, 2014). This is an apparent paradox as positive pressure would be required to drive gas back into solution or out of the conduit. The results of Wheeler *et al.* (2013) have cast some doubt on the ability of plants to refill embolized conduits while the bulk xylem water potential remains negative. However, it is clear from direct visualization that refilling occurs in some species over a timescale of hours (Brodersen *et al.*, 2010; Zwieniecki *et al.*, 2013). It is probable that this mechanism is most effective when transpiration is negligible, and that most refilling occurs at night or during periods of rain.

Currently, there is only a rudimentary understanding of how the ability to refill varies across species (Brodersen & McElrone, 2013). Although embolism repair has received considerable attention, published studies have focused on only a small number of species. A number of mechanisms have been proposed to explain the phenomenon of embolism refilling under tension, including osmotically driven flow (Hacke & Sperry, 2003), reverse osmosis from tissue pressure (Canny, 1997), and partial hydraulic isolation of refilling vessels (Zwieniecki & Holbrook, 2000). Most of the evidence suggests that this type of refilling is an active process that involves the xylem parenchyma and the phloem as sources of water and solutes (Zwieniecki & Holbrook, 2009; Nardini *et al.*, 2011). Given that xylem parenchyma appears to be essential for an active refilling process, it follows that species with lower parenchyma content in the xylem would have lower capacity to refill. On this basis it would be expected that the ability of gymnosperm species to refill would be limited, as they have very little xylem parenchyma (Johnson *et al.*, 2012). In fact, *c.* 95% of conifer xylem is composed of dead tracheids (Mauseth, 1988).

Evidence regarding the ability of gymnosperm species to refill is ambiguous. Seasonal patterns of stem hydraulic conductivity suggest that conifers can refill embolized tracheids after freeze-induced embolism occurs in the winter (Sperry *et al.*, 1994; McCulloh *et al.*, 2011; Mayr *et al.*, 2014). Whether gymnosperms can refill embolized tracheids on shorter timescales after drought is less certain. Some studies suggest that tracheids can be refilled if the xylem pressure reaches a critical threshold close to zero as determined by the Young–Laplace equation (Sobrado *et al.*, 1992). More recent studies indicate that a conifer species (*Callitris rhombodia*) could not refill embolized tracheids after drought, instead relying on regrowth of new xylem (Brodribb *et al.*, 2010). As a strategy for recovery from drought, regrowth of xylem has the obvious disadvantage that it occurs on a timescales of weeks to months, as opposed to refilling, which occurs on a timescale of hours.

A major limitation on progress in understanding of the patterns of embolism spread and mechanisms of embolism refilling is a lack of techniques that allow for noninvasive measurements at the appropriate scale. Recently, microCT has been developed as a method to assess the dynamics of embolism formation and refilling in great detail and in near real-time using three-dimensional (3D) time-lapse imaging (Brodersen, 2013; Brodersen *et al.*, 2010, 2013a; McElrone *et al.*, 2012, 2013).

In this study, the spatial patterns of xylem embolism were examined in saplings of a conifer species, *Sequoia sempervirens*, during cycles of drought and rewatering. This species is of great ecological and cultural significance in its native range, which consists of a narrow distribution along the coast of California. Recent studies indicate that fog has declined along the northern Californian coast, leaving fog-dependent vegetation such as coast redwoods at greater risk of mortality as climate change progresses (Limm *et al.*, 2009; Simonin *et al.*, 2009; Johnstone & Dawson, 2010). Given the vulnerability of vegetation to hydraulic failure during drought, a detailed understanding of processes governing embolism formation and repair in keystone species is essential (Choat *et al.*, 2012). Whether or not this

species is able to rapidly refill embolized conduits during recovery from drought stress may be an important component of its survival in a rapidly changing climate. To address the gap in our understanding of embolism spread and repair in gymnosperms we utilized microCT to examine the spread of embolism between tracheids in *S. sempervirens* saplings, and to test the hypothesis that this species is not capable of refilling embolism after drought stress.

Materials and Methods

MicroCT

Synchrotron-based microCT was utilized to visualize embolized and water-filled tracheids in the main stem axes of *Sequoia sempervirens* (Lamb. ex D. Don) Endl. saplings. Three-year-old saplings of *S. sempervirens* were purchased from Welker's Grove Nursery (California, USA) in September of 2010. Saplings were 30–40 cm in height growing in container pots of 0.5 l soil volume. Saplings were moved to a glasshouse at the UC Berkeley campus and maintained in a well-watered state for 2 wk before experiments. All saplings were transported to the Advanced Light Source (ALS), microtomography beamline 8.3.2, at the Lawrence Berkeley National Laboratories for 3 d in which the initial experiments were conducted.

The measurement protocol used to scan living plants is described in McElrone *et al.* (2013). In these experiments, water was withheld from 10 saplings for a period of 3 d before scanning. Stem water potential was estimated by covering leafy twigs in plastic wrap and aluminium foil for at least 30 min. Measurements were made just before scans using a Scholander Pressure Chamber (Plant Moisture Stress Model 600, Albany, OR, USA). MicroCT measurements were made in two periods during October 2010. In total, eight plants were scanned at the ALS beamline. Five plants were scanned to observe the spread of embolism within the xylem during dehydration. A further three plants were scanned during a cycle of drought and rehydration to determine if embolism repair occurs in this species.

Redwood saplings were placed in a custom-built aluminium holder and mounted on an air-bearing stage. The leaves and stem were covered by a 10-cm diameter Plexiglass cylinder to reduce vibrations by preventing foliage from contacting equipment during rotation of the stage. Saplings were scanned at 15 keV in the synchrotron X-ray beam while being rotated through 0–180° in increments of 0.25°. After each incremental rotation, the X-ray projection image was magnified through a series of lenses and relayed onto a 4 megapixel charge coupled device camera (#PCO 4000, Cooke Corp., Romulus, MI, USA). This yielded 720, two-dimensional (2D) projections per sample. Raw 2D tomographic projections were reconstructed into *c.* 500 sample TIF image slices using Octopus 8.3 software (Institute for Nuclear Sciences, University of Ghent, Belgium). The resulting images utilizing the ×2 lens yielded images with a 4.5 μm voxel resolution. These images were analysed in Avizo 8.1.1 software (VSG, Inc., Burlington, MA, USA) to determine the location of embolized tracheids and the cross-sectional area of embolized tracheids within each sample.

For each sapling, a 5 mm section of the main stem axis *c.* 3 cm above the soil surface was scanned before and after watering treatments. Droughted saplings were scanned after water potential measurements were made. Seedlings were then allowed to dry for a further 24 h while being scanned every 4–6 h. After this point, saplings were rewatered and allowed to recover from drought stress in a covered and humidified plastic container. Seedlings were scanned every 2–6 h during recovery from water stress. Covered leaf water potential was measured before each scan. Seedlings were then returned to the UC Berkeley glasshouse for a 2 wk period and maintained in well-watered conditions until the second set of experiments was performed on 21st October 2010. In the second scan session, saplings were scanned once to assess if tracheids had been refilled.

Samples of dried xylem tissue were also scanned at higher resolution in order to conduct more detailed analysis of connectivity between cell types. Stem tissue from one sapling was also dried in an oven at 40°C for 48 h to dehydrate the tissue for scanning at high magnification. This sample was mounted on the microCT sample stage and scanned using the 20× lens, yielding images with a voxel size of 0.325 μm. These images were then used to determine the number of tracheids within a subsample of wood tissue with direct connections to the ray cells using the 3D visualization software. In a wood sample with dimensions $175 \times 175 \times 500$ μm (1.53×10^7 μm^3), 260 tracheids were evaluated for ray cell connectivity. This was verified by identifying tracheids with visible pit connections to ray cells.

Light microscopy

Saplings were harvested after microCT observations were completed and stem segments in the region of the scan were preserved in 70% ethanol for microscopy. Sections were made on a Leica SM2010 sliding microtome (Leica Microsystems, Wetzlar, Germany). Sections were stained using toluidine blue (0.5% v/v) for 10 s before washing them with water and placing them on microscope slide. Light microscope images were acquired with an Olympus BX60 (Olympus America, Center Valley, PA, USA) at ×40, ×100 and ×200 magnification and imaged using a ProgRes C14 digital camera (Jenoptic, Jena, Germany). The total xylem area and tracheid dimensions were measured for each replicate plant using imageJ software (US National Institutes of Health, Bethesda, MD, USA).

Patterns of embolism spread with dehydration in redwood saplings were also assessed using dye uptake experiments. Saplings were purchased from Welker's Grove Nursery in August 2012 and moved to a glasshouse facility at UC Davis. All saplings were maintained in well-watered conditions for 2 wk. Before the beginning of experiments, saplings were divided into two groups for control (well watered) and drought treatment. Plants were brought to the laboratory and stems were excised underwater at the base of the stem and then recut underwater at 2 cm above the initial cut. Samples were then trimmed with a razor blade at the cut surface and allowed to

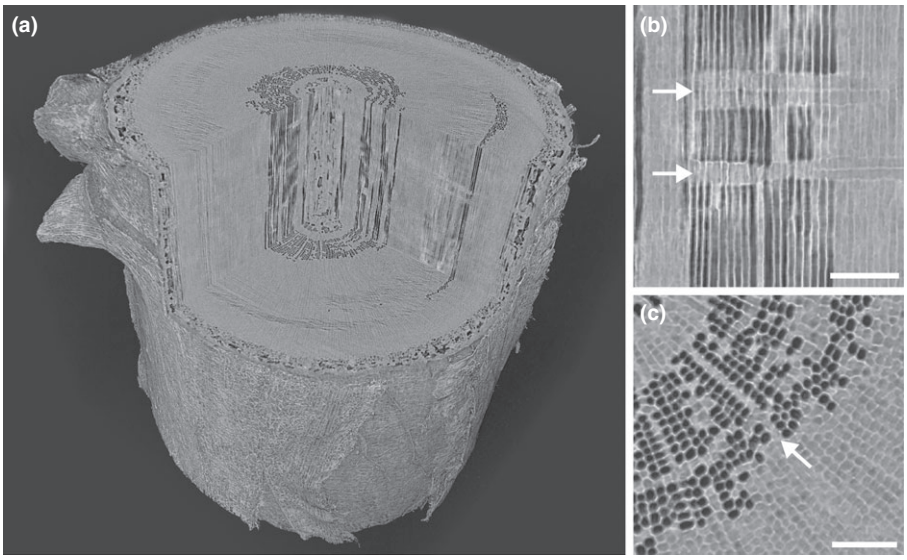

Fig. 1 Visualization of *Sequoia sempervirens* stem tissue from microcomputed tomography (microCT) scans. (a) Volume rendering with inner xylem tissue shown by cutaway. (b) Radial longitudinal slice from microCT scan. Embolized tracheids appear dark and water-filled tracheids appear grey. Rays (white arrows) can be seen passing in front of a file of embolized tracheids (c) Transverse slice from microCT of similar xylem section with gas-filled and water-filled tracheids. Rays (white arrows) can be seen interrupting a ring of embolized tracheids close to the pith. Bars, 100 μm. The stem water potential of this sample was −1.8 MPa at the time of scanning.

transpire for 30 min under ambient conditions in a solution of 0.5% Safranin O. Control plants were harvested after the initial 2 wk period. Drought plants were allowed to dry for 2–4 d while the covered leaf water potential was measured every day to track plant water status. Initial experiments indicated that significant cavitation occurred in these saplings at −1.8 MPa. After saplings attained this target water potential they were harvested for analysis of dye uptake. Samples were cut 5 cm above the initial cut point. The cut surfaces were cleaned with a razor blade and imaged at ×2.5 magnification using a dissecting microscope and a Nikon D40 digital SLR camera (Nikon Inc., Melville, NY, USA). Digital images were analysed using imageJ software to determine the proportion of stained and unstained xylem tissue in cross-section. Unstained tissue was assumed to be embolized and nonconductive. The percentage of embolized xylem relative to the whole cross-section was plotted onto the vulnerability curve generated from microCT scans.

Vulnerability to embolism analyses

A vulnerability to embolism curve was created by plotting the area of embolized conduits as a percentage of the total xylem area against stem water potential measured after the scan. Points from each of the eight samples were combined into one plot. Scans made after rewatering were excluded from the plot. A curve was fitted to the data using the methods of Pammenter & Vander Willigen (1998).

Results

Spread of embolism during dehydration

X-ray microCT allowed for excellent contrast between gas-filled and water-filled tracheids, providing a clear indication of where cavitation had occurred (Fig. 1). Ray parenchyma and parenchyma cells within the pith were also discernible in images (Fig. 1). Light microscopy revealed two complete growth rings defined by narrow bands of latewood tracheids (Fig. 2). MicroCT observations indicated that some embolism was invariably present in primary xylem conduits located directly adjacent to the pith (Fig. 3, Supporting Information, Fig. S1). Patches of embolized tracheids or individual embolized tracheids were also observed in the secondary xylem of some samples in initial scans (Fig. 4).

As the plants continued to dehydrate, further cavitation was observed in the outer sapwood of the stem. Cavitation events appeared to move in waves covering large proportions of the sapwood rather than as individual tracheids. These waves affected patches of connected tracheids and often occurred over the majority of a growth ring (Fig. 5a–c). Dye uptake experiments on droughted saplings revealed similar patterns of embolism spread to those observed with microCT (Fig. 5d–f). The vulnerability curve generated using data derived from microCT indicated that 50% of xylem area became embolized at a stem water potential of −1.81 MPa (Fig. 6). Embolism estimated from dye staining experiments was in close agreement with microCT observations.

In transverse 2D microCT slices of the xylem there appeared to be no direct connections between inner and outer rings containing embolized tracheids, thus initially suggesting that gas had 'jumped' between these rings. However, further analysis of the stem volume revealed that embolized tracheids in branch traces acted as connections between these rings (Fig. 7, Movie S1). It was also apparent that primary xylem conduits were directly connected to air-filled spaces within the pith, perhaps serving as reservoirs of air in these cases.

Recovery of samples after watering

Droughted plants reached a water potential of -1.41 ± 0.21 MPa (mean ± SE) before rewatering. After samples were rewatered, the stem water potential recovered to the well-watered status (-0.45 ± 0.06 MPa) within 8 h. However, scans showed no evidence of refilling at 24 h after rewatering

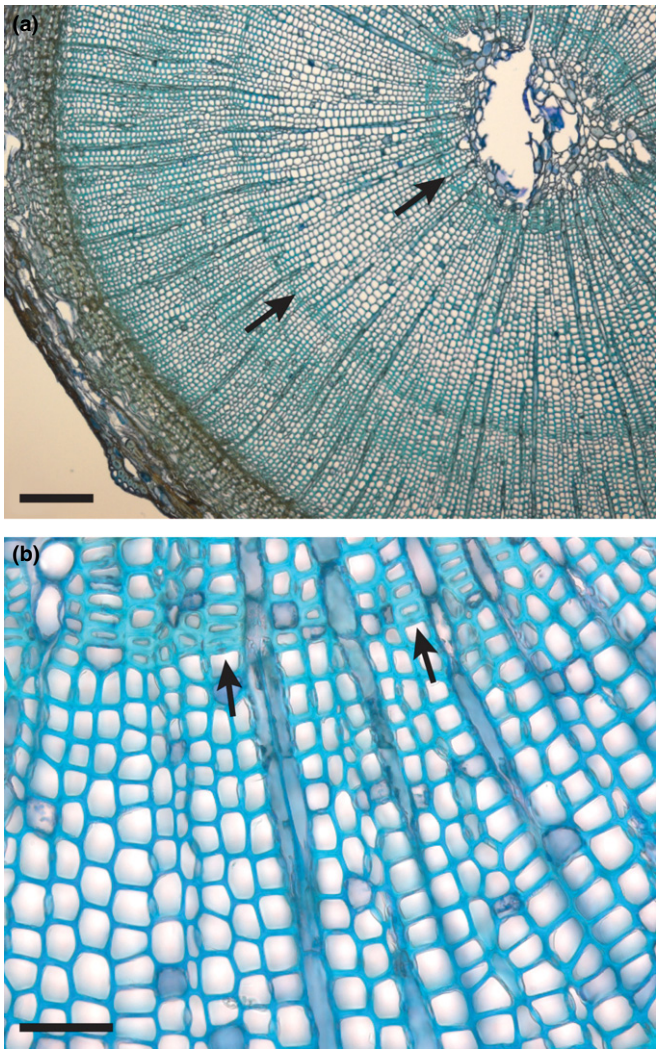

Fig. 2 Transverse sections from light microscopy show the xylem anatomy of *Sequoia sempervirens*. (a) Micrograph collected at ×40 magnification shows growth rings with the occurrence of a narrow band of latewood (arrows) at the end of each year. (b) Micrograph at ×200 magnification shows greater detail of tracheid structure, with narrow latewood tracheids (arrows) at the edge of the first year growth ring. Bars: (a) 250 μm; (b) 50 μm.

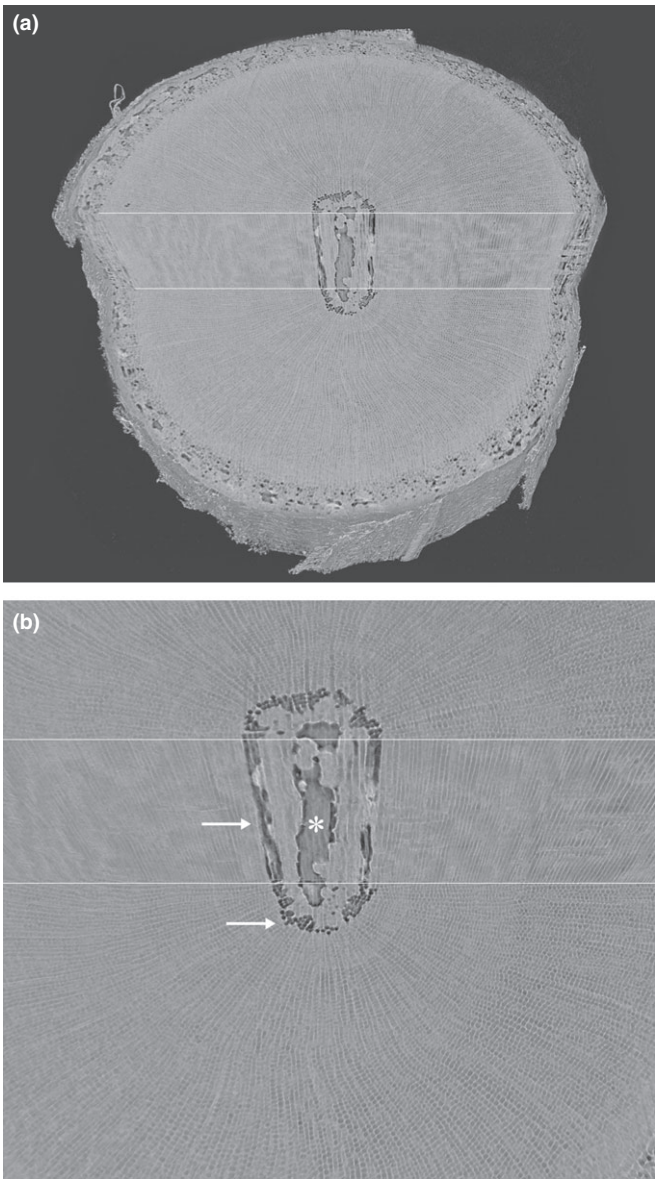

Fig. 3 Visualization of *Sequoia sempervirens* stem tissue from microcomputed tomography scans. (a) Volume rendering showing whole stem with cutaway exposing transverse and longitudinal planes within the xylem tissue. Air-filled primary xylem conduits (black) can be observed close to the pith. (b) Detail of (a) showing primary xylem conduits in transverse and longitudinal section (white arrows). Water-filled tracheids can be seen as a light grey colour directly adjacent to embolized tracheids. A large air space is visible within the pith (asterisk). White lines delineate the transverse and longitudinal planes. The stem water potential of this sample was −1.1 MPa at the time of scanning.

(Fig. 8b). After 2 wk under well-watered conditions, there was also no evidence of refilling, although stem water potential had recovered to –0.22 ± 0.03 MPa in all samples (Fig. 8c).

Although refilling was not observed, connections between tracheids and ray parenchyma cells were abundant. Every tracheid visualized at 325 nm image resolution showed evidence of a direct connection to ray cells (i.e. pitting in the tracheid walls connecting them to the ray cells). The rays were distributed within the xylem such that all tracheids observed were in contact with at least one band of ray tissue, and many tracheids had contact with two or more rays (Fig. 9).

Discussion

This study provides the first noninvasive visualization of embolism formation and spread in the xylem of conifers. These observations suggest that air seeding between bordered pits is the primary mechanism of embolism spread in this species. However, the occurrence of isolated embolized tracheids suggests that other mechanisms of nucleation operate in the xylem of this species. MicroCT observations revealed no evidence of refilling in *S. sempervirens* during a cycle of drought and recovery, suggesting that this species does not possess a mechanism that allows for rapid refilling of tracheids after drought.

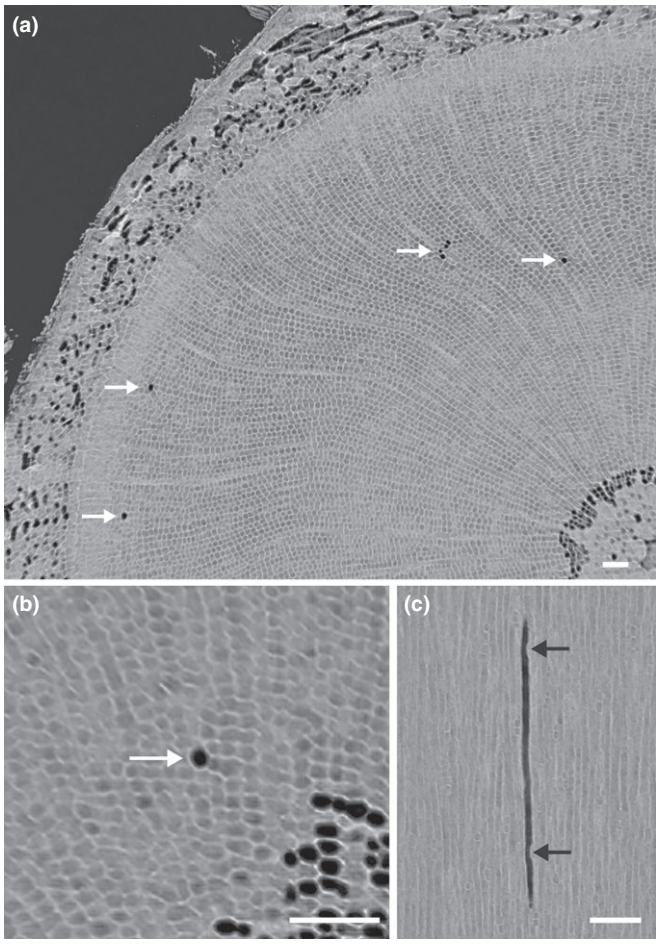

Fig. 4 Isolated embolized tracheids in the stem xylem of *Sequoia sempervirens*. (a) Transverse slice shows an embolized tracheid (white arrows) surrounded by water-filled tracheids. (b) Detail of isolated embolized tracheid in transverse section. (c) A tangential longitudinal slice confirming that the embolized tracheid is isolated from other gas-filled cells. Ray cells directly adjacent to the tracheid (black arrows) appear as protrusions in the tracheid walls. Bars, 100 μm.

Spread of embolism in the xylem with increasing water stress

The majority of samples initially contained some embolized tracheids in close proximity to the pith. These appeared to be primary xylem conduits that were formed during the initial extension growth of the stem. It is assumed that these conduits become embolized during or after extension growth as they are stretched and ruptured (Tyree & Sperry, 1989). A similar pattern was observed in a vessel-bearing species, *Vitis vinifera*, using both magnetic resonance imaging and microCT (Choat *et al.*, 2010; Brodersen *et al.*, 2013a). In grapevine, embolism spread outwards from the pith towards the cambium via direct connections and xylem vessel relays between vessels (Brodersen *et al.*, 2013a,b). In *S. sempervirens*, embolism did not propagate along radial sectors as observed in grapevine. Instead, embolism spread roughly within growth rings of the stem in the tangential direction, with ray parenchyma providing no barrier to air seeding. This was explained by observations on dried samples of *S. sempervirens*, which clearly showed that many of the tracheids wrap around the rays, with connections to other tracheids both above and below ray cells (Fig. 9).

Although 3–6 h elapsed between scans, it appeared that cavitation spread very rapidly through a growth ring of the xylem once nucleated. Serendipitously, one of the scans was made during the time that cavitation was occurring in the xylem (Fig. S2). Given that the scans during this experiment were 12 min in duration, it was apparent that embolism spread rapidly around the outer growth ring once critical xylem water potentials were reached. Thus, embolism in a highly connected tracheid-based xylem seems to operate on an 'all or nothing' principle, where up to 40% of conductive tracheids are lost in a single cavitation event. As expected from these observations, saplings had steep vulnerability curves, with loss of conductance occurring rapidly once the inflection point of the sigmoidal curve was reached (Fig. 6).

The difference in directionality of embolism spread may be derived from the orientation of bordered pit connections

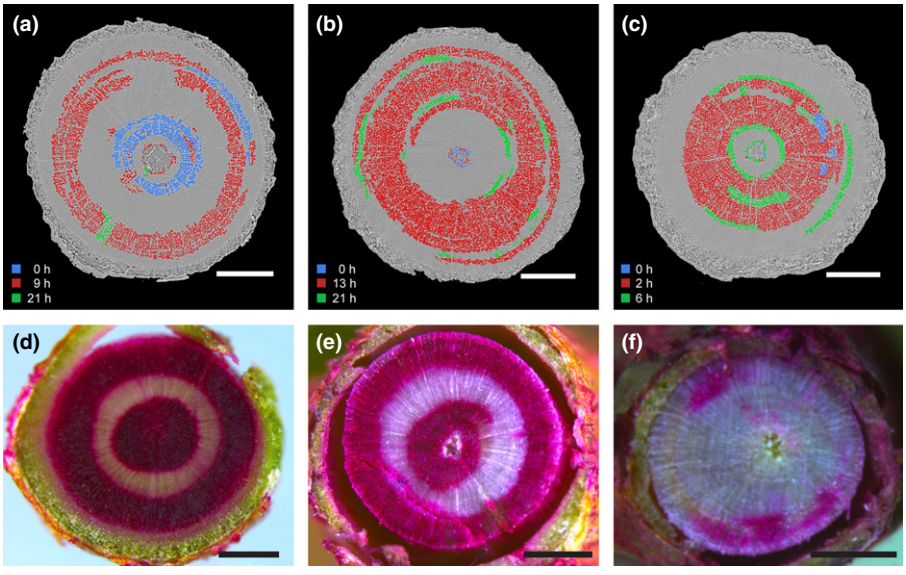

Fig. 5 Transverse slices from microcomputed tomography (microCT) and dye staining show the spatial and temporal patterns of embolism formation in the stem xylem of *Sequoia sempervirens* saplings during natural dehydration. (a–c) The progression of embolism formation observed with microCT is shown in three replicate plants with colours indicating the occurrence of embolism in the xylem and the time point of scanning (in h). Each replicate plant was scanned three times in succession (d–f) Patterns of embolism in three replicate stems shown by dye staining with safranin O. Xylem area not stained was embolized. Bars, 500 μm.

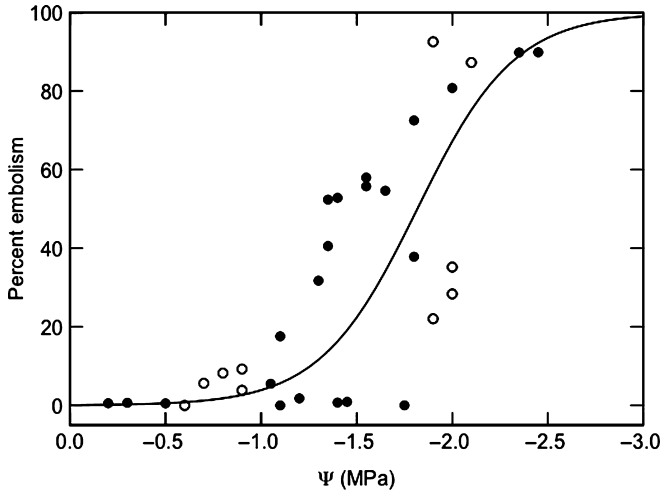

Fig. 6 Vulnerability to embolism curve for stem xylem of *Sequoia sempervirens* saplings. The relationship between percentage area of embolized xylem and stem water potential was obtained from microcomputed tomography (microCT; closed symbols) and dye staining (open symbols) observations. MicroCT data were fitted with an exponential sigmoidal equation Percent embolism = $100/(1 + \exp(a(\Psi - b)))$.

between conduits in *V. vinifera* and *S. sempervirens*. In conifers, most of the bordered pit connections occur on the radial walls of the tracheids (Mauseth, 1988). Observations of dried samples at high resolution indicated that 96% of pits were observed on the radial tracheid walls of *S. sempervirens* saplings (Fig. 9). Therefore, it is far more likely for air seeding to proceed in the tangential direction, that is, around the growth ring. In grapevine, the majority of intervessel connections are oriented in the radial direction, allowing air seeding to occur preferentially along sectors from pith to cambium (Brodersen *et al.*, 2013a,b).

From observations of single transverse slices of sapwood, it appeared that embolism 'jumped' between growth rings of *S. sempervirens*, implying that cavitation was not nucleated by air seeding (Fig. 5a). However, three-dimensional analyses of scan volumes revealed that apparently isolated patches of embolized tracheids were connected by branch traces in which many of conduits were embolized (Fig. 7, Movie S1). It appears that these branch traces form a weak point that allows gas to spread more widely in the network of tracheids, although the mechanism by which the conduits in these branch traces initially became air-filled remains uncertain. One possibility is that gas leaked from air-filled spaces in the pith into ruptured protoxylem conduits and then into the primary xylem connected to branch traces. This is supported by connections observed between air spaces in the pith and primary xylem conduits (Fig. 7). A second possibility is that air moved into branch trace xylem from the outside when branches were damaged. Some minor branches were removed from the stems before experiments to provide a more regular surface for scanning and this may have provided an air entry point. Although in this case branches were removed as part of experimental protocol, damage to leaves and branches would be common under natural conditions as a result of herbivory or mechanical damage. In

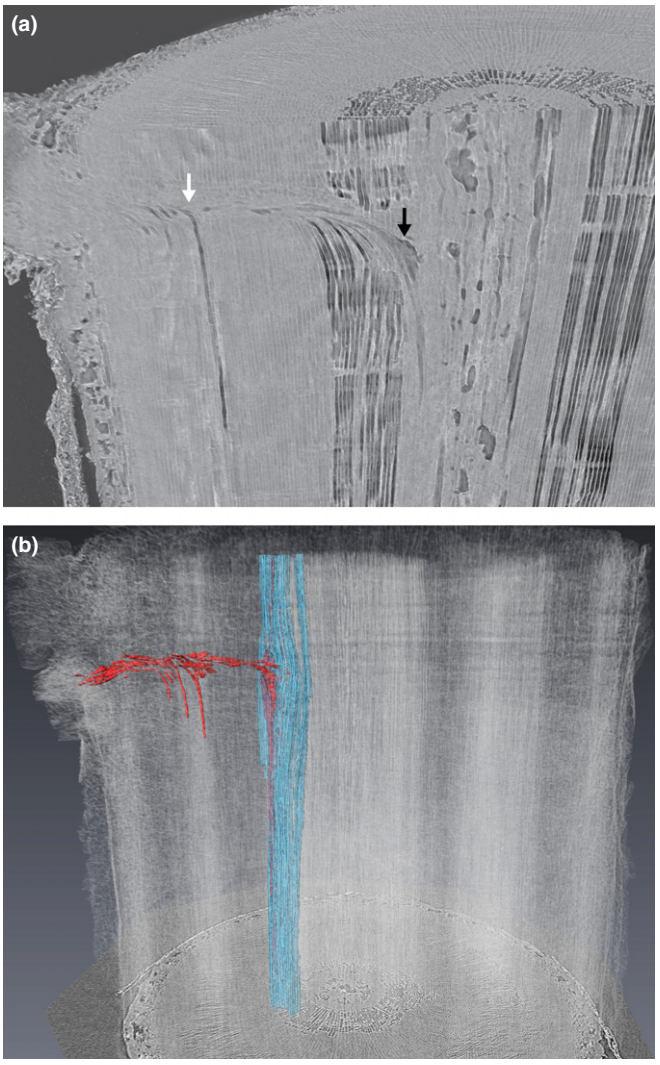

Fig. 7 Volume renderings from microcomputed tomography (microCT) scan showing details of branch traces in the stem xylem of *Sequoia sempervirens*. (a) Longitudinal face showing a series of connected embolized conduits in a branch trace running from the pith to the outside of the stem. Direct connections between embolized conduits in the branch trace and tracheids in the outer growth rings can be seen in this plane (white arrow). Connections between primary xylem conduits leading to the branch trace and air-filled spaces in the pith are also apparent (black arrow). (b) Embolized tracheids in the branch trace are identified in red, showing connections between xylem conduits. Embolized conduits from the inner ring of secondary xylem are shown in blue.

fact, this was hypothesized to be a potential source of air in the original statement of the air seeding hypothesis (Zimmermann, 1983; Tyree & Sperry, 1989). Further experimentation is required to elucidate the role of air spaces in the pith, which are commonly observed in samples using microCT.

In some cases, isolated embolized tracheids were observed in the xylem, raising the question of how cavitation was nucleated in these instances (Fig. 4). In the absence of obvious damage to the xylem in the region of these tracheids, it is possible that air was drawn into these tracheids from intercellular air spaces. However, no air spaces could be observed directly adjacent to these tracheids. Other mechanisms include homogeneous nucleation

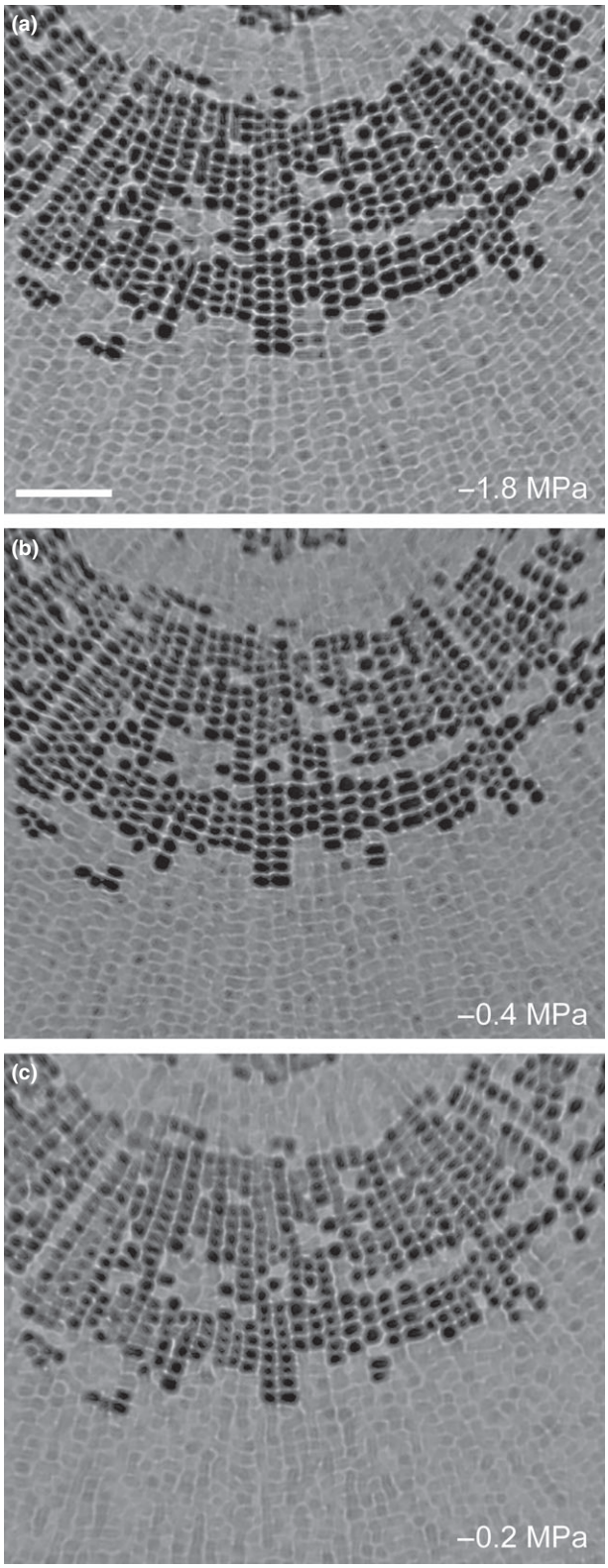

Fig. 8 Transverse slices from microcomputed tomography (microCT) scans of *Sequoia sempervirens* stem showing the functional status of tracheids during a cycle of drought and rewatering. The covered leaf water potential at each time point is shown at the bottom right of each panel. The slices show xylem tissue at three different time points: (a) the initial scan after the plant was subjected to mild drought stress; (b) 24 h after rewatering; and (c) after 2 wk at favourable water status. Bar, 100 μm (for all images).

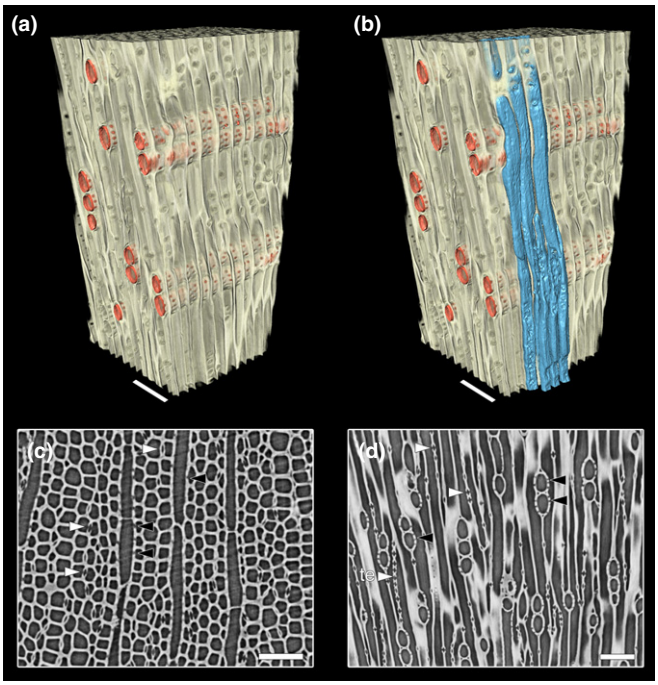

Fig. 9 Microcomputed tomography (microCT) volume renderings and two-dimensional (2D) image slices show connections between the rays and tracheids in the xylem tissue of *Sequoia sempervirens* saplings, revealing dense pitting between rays (orange) and tracheids (three-dimensional lumen is rendered blue in b). Many tracheids had connections with two or more rays and most tracheid–tracheid connections were in the radial direction. Black arrowheads point to ray–tracheid pitting in (c) and (d), while white arrows point to tracheid–tracheid pitting. te, tracheid ending in (d). Bars: (a, b) 150 μm; (c, d) 100 μm.

or nucleation from hydrophobic cracks (Pickard, 1981; Zwieniecki & Holbrook, 2009). Homogeneous nucleation remains extremely unlikely at the pressures present in the xylem sap of these saplings (Oertli, 1971; Pickard, 1981). It is possible that defects in the walls of these tracheids may have allowed cavitation at very mild tensions. Regardless of the mechanism, it appears that these isolated, embolized tracheids are important as a source of air from which air seeding can occur when the critical tension necessary to displace the pit membrane tori is reached. However, it is also clear that this mechanism of nucleation is restricted to a very few tracheids, because otherwise air seeding through pit membranes would not be expected to play a major role in the spread of embolism. This is consistent with the observations of Ponomarenko *et al.* (2014), who reported both air seeding and within-tracheid nucleation in a thin section of conifer xylem observed by light microscope during dehydration.

The patterns of embolism spread observed with microCT were consistent with the results of previous physiological and anatomical measurements, indicating that latewood tracheids begin to cavitate before earlywood tracheids as xylem tension increases (Domec & Gartner, 2002; Domec *et al.*, 2006). MicroCT visualizations of *S. sempervirens* revealed that latewood tracheids, generally those closest to the pith, became embolized before earlywood tracheids (Figs 5, S1). In other conifer species, the lower cavitation resistance of latewood tracheids has been explained by pit membrane characteristics (Domec *et al.*, 2006); latewood tracheids tend to have larger

and less flexible margo strands, meaning that the membrane is not easily displaced, preventing the torus from sealing over the pit aperture (Gregory & Petty, 1973; Domec *et al.*, 2006). The transition zone between earlywood and latewood tracheids appeared to act as a point of resistance for embolism spread, with latewood tracheids cavitating before earlywood tracheids. Previous anatomical work on conifers indicates that pits occur on tangential walls of tracheids at the growth ring boundary between latewood and earlywood tracheids (Koran, 1977; Kitin *et al.*, 2009). This allows for radial movement of fluid, but also provides a pathway by which gas can penetrate between growth rings. The observation that embolism was contained within growth rings of *S. sempervirens* suggests that these tangential wall pits may be more resistant to air seeding, although this remains to be confirmed by cell ultrastructural studies.

No evidence for refilling after rehydration

Previous studies of refilling support the theory that conifers lack a mechanism to rapidly refill embolized tracheids after drought (Brodersen & McElrone, 2013). While a number of studies report seasonal refilling in conifers (Sperry *et al.*, 1994; McCulloh *et al.*, 2011; Mayr *et al.*, 2014), direct visualization of xylem using cryo-scanning electron microscopy did not provide any evidence of springtime refilling in three conifer species (Utsumi *et al.*, 2003).

Evidence for refilling on shorter timescales (h) after drought is scant. Studies on detached branches of *Pinus sylvestris* that were connected to a water source indicated that tracheids were refilled only at pressures > −0.04 MPa (Sobrado *et al.*, 1992). In this case, water may have been drawn into embolized tracheids by surface tension generated at the curved menisci inside tracheids. The relevance of refilling in detached branches to embolism repair in intact conifers remains to be seen. More recently, Laur & Hacke (2014) report refilling on a timescale of hours in *Picea glauca* saplings exposed to drought and rewatering. This suggests that refilling after drought is possible in some conifer species.

We saw no evidence for embolism refilling in tracheids after drought on timescales of hours, days and weeks. This is consistent with recent work on *Callitris* species, which demonstrated that these species did not refill embolized tracheids after the imposition of severe drought stress (Brodribb *et al.*, 2010). Instead, recovery of leaf gas exchange took place over a period of months and relied upon growth of new xylem tissue. In the present study, stem water potential recovered within 24 h of rewatering, but no change was observed in gas-filled tracheids after 2 wk, indicating that drought-induced embolism is not reversible in *S. sempervirens* saplings.

There are a number of possible explanations as to why refilling does not occur in *S. sempervirens* after drought. It is possible that the tori of bordered pit membranes become permanently sealed to the outer pit aperture after embolism has occurred (Siau, 1984). However, the results of Mayr *et al.* (2014) indicate that aspiration of tori is fully reversible in *Picea abies* after winter embolism. It is also true that conifers lack the abundant xylem parenchyma that is believed to drive refilling in angiosperm species (Salleo *et al.*, 2004; Johnson *et al.*, 2012). In this context, it should not be surprising that a conifer species lacks an active refilling mechanism, as their xylem appears to lack the specialization in cell function necessary for such a process as observed in angiosperms. However, despite the overall low proportion of parenchyma in the xylem, we observed that every tracheid had at least one connection with ray parenchyma cell (Fig. 9). This is consistent with observations for three conifer species by Zhang *et al.* (2003). It was also clear that the ray parenchyma cells remained hydrated while surrounding tracheids became embolized (Fig. 4C). It would thus be theoretically possible for tracheids to be refilled by ray parenchyma cells, although the very small volume of parenchyma cells relative to tracheids is likely to place significant limitations on the extent to which refilling can occur.

Ecological implications for the distribution of *S. sempervirens*

The natural distribution of *S. sempervirens* is limited to a narrow coastal zone of California and is strongly associated with the occurrence of summer marine fogs (Johnstone & Dawson, 2010). In addition to the effects of fog on soil moisture (i.e. condensation and drip), field observations and controlled experiments indicate that fog can be intercepted directly by the canopy of *S. sempervirens* and absorbed into the needles (Burgess & Dawson, 2004; Simonin *et al.*, 2009). This foliar water uptake can effectively decouple leaf water potential from soil water status and assist in maintaining higher photosynthetic rates. Climate analyses indicate a 33% reduction in fog frequency along the coast of California since the early 20th century (Johnstone & Dawson, 2010). This reduction in fog frequency is likely to continue into the future, exposing *S. sempervirens* forests on the coast of California to increasing drought stress. This is exacerbated by the poor stomatal control exhibited by gymnosperms in response to increased evaporative demand, which can also result in significant night-time transpiration (Burgess & Dawson, 2004). Our results suggest that *S. sempervirens* will have difficulty recovering from increased drought stress because it lacks a mechanism to facilitate embolism repair after drought. This may be particularly problematic during severe heat waves that cause significant xylem embolism in a short time frame.

Tree saplings are often considered the most vulnerable life history stage to drought-induced mortality given their low rooting volume (McDowell *et al.*, 2008). In this context, we note that branches of mature *S. sempervirens* trees have significantly higher resistance to embolism than the saplings used in our experiments (Burgess *et al.*, 2006; Pittermann *et al.*, 2010) and currently maintain significant hydraulic safety margins during typical periods of transpiration. The impact of decreased fog will be dictated by the magnitudes of declines in stem water potential and how close this brings the plant to the hydraulic point of no return (Simonin *et al.*, 2009). The results of the present study have implications for sapling establishment and therefore future generations of coast redwood trees.

Acknowledgements

We thank D. Parkinson and A. MacDowell for their assistance at the Lawrence Berkeley National Laboratory ALS beamline 8.3.2

microtomography facility. Danielle Creek is thanked for assistance with light microscopy, and Amr Zedan and Zainab Nasafi for assistance with image analysis. This work was supported by the National Science Foundation (grant no. 0818479) and US Department of Agriculture-Agricultural Research Service Current Research Information System funding (research project no. 5306–21220–004–00). The ALS is supported by the Director, Office of Science, Office of Basic Energy Sciences, of the US Department of Energy (contract no. DE–AC02–05CH11231). B.C. acknowledges travel funding from the International Synchrotron Access Program (ISAP) managed by the Australian Synchrotron. The ISAP is an initiative of the Australian government being conducted as part of the National Collaborative Research Infrastructure Strategy.

References

Ameglio T, Ewers FW, Cochard H, Martignac M, Vandame M, Bodet C, Cruiziat P. 2001. Winter stem xylem pressure in walnut trees: effects of carbohydrates, cooling and freezing. *Tree Physiology* **21**: 387–394.

Bailey IW. 1913. The preservative treatment of wood – II. The structure of the pit membranes in the tracheids of Cconifers and their relation to the penetration of Ggases, liquids, and finely divided solids into green and seasoned wood. *Journal of Forestry* **11**: 12–20.

Briggs LJ. 1950. Limiting negative pressure of water. *Journal of Applied Physics* **21**: 721–722.

Brodersen CR. 2013. Using high resolution computed tomography to visualize the three dimensional structure and function of plant vasculature. *IAWA Journal* **34**: 408–424.

Brodersen CR, Choat B, Chatelet DS, Shackel KA, Matthews MA, McElrone AJ. 2013a. Xylem vessel relays contribute to radial connectivity in grapevine stems (*Vitis vinifera* and *V. arizonica*; Vitaceae). *American Journal of Botany* **100**: 314–321.

Brodersen CR, McElrone AJ. 2013. Maintenance of xylem network transport capacity: a review of embolism repair in vascular plants. *Frontiers in Plant Science* **4**: 108.

Brodersen CR, McElrone AJ, Choat B, Lee EF, Shackel KA, Matthews MA. 2013b. *In vivo* visualizations of drought-induced embolism spread in *Vitis vinifera*. *Plant Physiology* **161**: 1820–1829.

Brodersen CR, McElrone AJ, Choat B, Matthews MA, Shackel KA. 2010. The dynamics of embolism repair in xylem: *in vivo* visualizations using high resolution computed tomography. *Plant Physiology* **154**: 1088–1095.

Brodribb TJ, Bowman DMJS, Nichols S, Delzon S, Burlett R. 2010. Xylem function and growth rate interact to determine recovery rates after exposure to extreme water deficit. *New Phytologist* **188**: 533–542.

Brodribb TJ, Cochard H. 2009. Hydraulic failure defines the recovery and point of death in water-stressed conifers. *Plant Physiology* **149**: 575–584.

Burgess SSO, Dawson TE. 2004. The contribution of fog to the water relations of *Sequoia sempervirens* (D. Don): foliar uptake and prevention of dehydration. *Plant, Cell & Environment* **27**: 1023–1034.

Burgess SSO, Pittermann J, Dawson TE. 2006. Hydraulic efficiency and safety of branch xylem increases with height in *Sequoia sempervirens* (D. Don) crowns. *Plant, Cell & Environment* **29**: 229–239.

Canny MJ. 1997. Vessel contents during transpiration – embolisms and refilling. *American Journal of Botany* **84**: 1223–1230.

Choat B. 2013. Predicting thresholds of drought-induced mortality in woody plant species. *Tree Physiology* **33**: 669–671.

Choat B, Cobb AR, Jansen S. 2008. Structure and function of bordered pits: new discoveries and impacts on whole-plant hydraulic function. *New Phytologist* **177**: 608–625.

Choat B, Drayton WM, Brodersen C, Matthews MA, Shackel KA, Wada H, McElrone AJ. 2010. Measurement of vulnerability to water stress-induced cavitation in grapevine: a comparison of four techniques applied to a long-vesseled species. *Plant, Cell & Environment* **33**: 1502–1512.

Choat B, Jansen S, Brodribb TJ, Cochard H, Delzon S, Bhaskar R, Bucci SJ, Feild TS, Gleason SM, Hacke UG *et al.* 2012. Global convergence in the vulnerability of forests to drought. *Nature* **491**: 752–755.

Choat B, Jansen S, Zwieniecki MA, Smets E, Holbrook NM. 2004. Changes in pit membrane porosity due to deflection and stretching: the role of vestured pits. *Journal of Experimental Botany* **55**: 1569–1575.

Choat B, Pittermann J. 2009. New insights into bordered pit structure and cavitation resistance in angiosperms and conifers. *New Phytologist* **182**: 557–560.

Cobb AR, Choat B, Holbrook NM. 2007. Dynamics of freeze–thaw embolism in *Smilax rotundifolia* (Smilacaceae). *American Journal of Botany* **94**: 640–649.

Debenedetti PG. 2013. Physics of water stretched to the limit. *Nature Physics* **9**: 7–8.

Delzon S, Douthe C, Sala A, Cochard H. 2010. Mechanism of water-stress induced cavitation in conifers: bordered pit structure and function support the hypothesis of seal capillary-seeding. *Plant, Cell & Environment* **33**: 2101–2111.

Dixon HH, Joly J. 1895. On the ascent of sap. *Philosophical Transactions of the Royal Society of London B* **186**: 563–576.

Domec JC, Gartner BL. 2002. Age- and position-related changes in hydraulic versus mechanical dysfunction of xylem: inferring the design criteria for Douglas-fir wood structure. *Tree Physiology* **22**: 91–104.

Domec JC, Lachenbruch B, Meinzer FC. 2006. Bordered pit structure and function determine spatial patterns of air-seeding thresholds in xylem of Douglas fir (*Pseudotsuga menziesii*; Pinaceae) trees. *American Journal of Botany* **93**: 1588–1600.

Gregory SC, Petty JA. 1973. Valve action of bordered pits in conifers. *Journal of Experimental Botany* **24**: 763–767.

Hacke UG, Sperry JS. 2003. Limits to xylem refilling under negative pressure in *Laurus nobilis* and *Acer negundo*. *Plant, Cell & Environment* **26**: 303–311.

Hacke UG, Sperry JS, Pittermann J. 2004. Analysis of circular bordered pit function – II. Gymnosperm tracheids with torus-margo pit membranes. *American Journal of Botany* **91**: 386–400.

Holbrook NM, Zwieniecki MA. 1999. Embolism repair and xylem tension: do we need a miracle? *Plant Physiology* **120**: 7–10.

Jansen S, Lamy JB, Burlett R, Cochard H, Gasson P, Delzon S. 2012. Plasmodesmatal pores in the torus of bordered pit membranes affect cavitation resistance of conifer xylem. *Plant, Cell & Environment* **35**: 1109–1120.

Johnson DM, McCulloh KA, Woodruff DR, Meinzer FC. 2012. Hydraulic safety margins and embolism reversal in stems and leaves: why are conifers and angiosperms so different? *Plant Science* **195**: 48–53.

Johnstone JA, Dawson TE. 2010. Climatic context and ecological implications of summer fog decline in the coast redwood region. *Proceedings of the National Academy of Sciences, USA* **107**: 4533–4538.

Kitin P, Fujii T, Abe H, Takata K. 2009. Anatomical features that facilitate radial flow across growth rings and from xylem to cambium in *Cryptomeria japonica*. *Annals of Botany* **103**: 1145–1157.

Koran Z. 1977. Tangential pitting in black spruce tracheids. *Wood Science and Technology* **11**: 115–123.

Laur J, Hacke UG. 2014. Exploring *Picea glauca* aquaporins in the context of needle water uptake and xylem refilling. *New Phytologist* **203**: 388–400.

Limm EB, Simonin KA, Bothman AG, Dawson TE. 2009. Foliar water uptake: a common water acquisition strategy for plants of the redwood forest. *Oecologia* **161**: 449–459.

Martorell S, Diaz-Espejo A, Medrano H, Ball MC, Choat B. 2014. Rapid hydraulic recovery in *Eucalyptus pauciflora* after drought: linkages between stem hydraulics and leaf gas exchange. *Plant, Cell & Environment* **37**: 617–626.

Mauseth JD. 1988. *Plant anatomy*. California, CA, USA: Benjamin/Cummings Publishing Company.

Mayr S, Schmid P, Laur J, Rosner S, Charra-Vaskou K, Dämon B, Hacke UG. 2014. Uptake of water via branches helps timberline conifers refill embolized xylem in late winter. *Plant Physiology* **164**: 1731–1740.

McCulloh KA, Johnson DM, Meinzer FC, Lachenbruch B. 2011. An annual pattern of native embolism in upper branches of four tall conifer species. *American Journal of Botany* **98**: 1007–1015.

McCully ME. 1999. Root xylem embolisms and refilling. Relation to water potentials of soil, roots, and leaves, and osmotic potentials of root xylem sap. *Plant Physiology* **119**: 1001–1008.

McDowell N, Pockman WT, Allen CD, Breshears DD, Cobb N, Kolb T, Plaut J, Sperry J, West A, Williams DG *et al.* 2008. Mechanisms of plant survival and mortality during drought: why do some plants survive while others succumb to drought? *New Phytologist* **178**: 719–739.

McElrone AJ, Brodersen CR, Alsina MM, Drayton WM, Matthews MA, Shackel KA, Wada H, Zufferey V, Choat B. 2012. Centrifuge technique consistently overestimates vulnerability to water stress-induced cavitation in grapevines as confirmed with high-resolution computed tomography. *New Phytologist* **196**: 661–665.

McElrone AJ, Choat B, Parkinson DY, MacDowell AA, Brodersen CR. 2013. Using high resolution computed tomography to visualize the three dimensional structure and function of plant vasculature. *Journal of Visualized Experiments* **74**: doi: 10.3791/50162.

Melcher PJ, Meinzer FC, Yount DE, Goldstein G, Zimmermann U. 1998. Comparative measurements of xylem pressure in transpiring and non-transpiring leaves by means of the pressure chamber and the xylem pressure probe. *Journal of Experimental Botany* **49**: 1757–1760.

Milburn JA. 1973. Cavitation studies on whole ricinus plants by acoustic detection. *Planta* **112**: 333–342.

Nardini A, Lo Gullo MA, Salleo S. 2011. Refilling embolized xylem conduits: is it a matter of phloem unloading? *Plant Science* **180**: 604–611.

Oertli JJ. 1971. Stability of water under tension in xylem. *Zeitschrift Fur Pflanzenphysiologie* **65**: 195–209.

Pammenter NW, Vander Willigen C. 1998. A mathematical and statistical analysis of the curves illustrating vulnerability of xylem to cavitation. *Tree Physiology* **18**: 589–593.

Pickard WF. 1981. The ascent of sap in plants. *Progress in Biophysics & Molecular Biology* **37**: 181–229.

Pittermann J, Choat B, Jansen S, Stuart SA, Lynn L, Dawson TE. 2010. The relationships between xylem safety and hydraulic efficiency in the Cupressaceae: the evolution of pit Membrane form and function. *Plant Physiology* **153**: 1919–1931.

Pittermann J, Sperry JS, Hacke UG, Wheeler JK, Sikkema EH. 2005. Torus-margo pits help conifers compete with angiosperms. *Science* **310**: 1924.

Pockman WT, Sperry JS, Oleary JW. 1995. Sustained and significant negative water-pressure in xylem. *Nature* **378**: 715–716.

Ponomarenko A, Vincent O, Pietriga A, Cochard H, Badel É, Marmottant P. 2014. Ultrasonic emissions reveal individual cavitation bubbles in water-stressed wood. *Journal of the Royal Society Interface* **11**: 20140480.

Salleo S, Lo Gullo MA, Trifilo P, Nardini A. 2004. New evidence for a role of vessel-associated cells and phloem in the rapid xylem refilling of cavitated stems of *Laurus nobilis* L. *Plant, Cell & Environment* **27**: 1065–1076.

Salleo S, LoGullo MA, DePaoli D, Zippo M. 1996. Xylem recovery from cavitation-induced embolism in young plants of *Laurus nobilis*: a possible mechanism. *New Phytologist* **132**: 47–56.

Siau JF. 1984. *Transport processes in wood*. Berlin, Germany: Springer-Verlag.

Simonin KA, Santiago LS, Dawson TE. 2009. Fog interception by *Sequoia sempervirens* (D. Don) crowns decouples physiology from soil water deficit. *Plant, Cell & Environment* **32**: 882–892.

Sobrado MA, Grace J, Jarvis PG. 1992. The limits to xylem embolism recovery in *Pinus sylvestris* L. *Journal of Experimental Botany* **43**: 831–836.

Sperry JS, Holbrook NM, Zimmermann MH, Tyree MT. 1987. Spring filling of xylem vessels in wild grapevine. *Plant Physiology* **83**: 414–417.

Sperry JS, Nichols KL, Sullivan JEM, Eastlack SE. 1994. Xylem embolism in ring-porous, diffuse-porous, and coniferous trees of northern Utah and interior Alaska. *Ecology* **75**: 1736–1752.

Sperry JS, Tyree MT. 1988. Mechanism of water stress-induced xylem embolism. *Plant Physiology* **88**: 581–587.

Sperry JS, Tyree MT. 1990. Water stress-induced xylem embolism in 3 species of conifers. *Plant, Cell & Environment* **13**: 427–436.

Stiller V, Sperry JS, Lafitte R. 2005. Embolized conduits of rice (*Oryza sativa*, Poaceae) refill despite negative xylem pressure. *American Journal of Botany* **92**: 1970–1974.

Tyree MT, Salleo S, Nardini A, Lo Gullo MA, Mosca R. 1999. Refilling of embolized vessels in young stems of laurel. Do we need a new paradigm? *Plant Physiology* **120**: 11–21.

Tyree MT, Sperry JS. 1989. Vulnerability of xylem to cavitation and embolism. *Annual Review of Plant Physiology and Plant Molecular Biology* **40**: 19–38.

Tyree MT, Zimmermann MH. 2002. *Xylem structure and the ascent of sap*. New York, NY, USA: Springer-Verlag.

Urli M, Porte AJ, Cochard H, Guengant Y, Burlett R, Delzon S. 2013. Xylem embolism threshold for catastrophic hydraulic failure in angiosperm trees. *Tree Physiology* **33**: 672–683.

Utsumi Y, Sano Y, Funada R, Ohtani J, Fujikawa S. 2003. Seasonal and perennial changes in the distribution of water in the sapwood of conifers in a sub-frigid zone. *Plant Physiology* **131**: 1826–1833.

Wei CF, Tyree MT, Steudle E. 1999. Direct measurement of xylem pressure in leaves of intact maize plants. A test of the cohesion-tension theory taking hydraulic architecture into consideration. *Plant Physiology* **121**: 1191–1205.

Wheeler JK, Huggett BA, Tofte AN, Rockwell FE, Holbrook NM. 2013. Cutting xylem under tension or supersaturated with gas can generate PLC and the appearance of rapid recovery from embolism. *Plant, Cell & Environment* **36**: 1938–1949.

Wheeler TD, Stroock AD. 2008. The transpiration of water at negative pressures in a synthetic tree. *Nature* **455**: 208–212.

Zhang C, Fujita M, Takabe K. 2003. Contact and non-contact proportions between axial elements and rays. *IAWA Journal* **24**: 247–255.

Zheng Q, Durben DJ, Wolf GH, Angell CA. 1991. Liquids at large negative pressures - water at the homogeneous nucleation limit. *Science* **254**: 829–832.

Zimmermann MH. 1983. *Xylem structure and the ascent of sap*. New York, NY, USA: Springer-Verlag.

Zimmermann MH, Brown CL. 1971. *Trees: structure and function*. New York, NY, USA; Berlin, Heidelberg, Germany: Springer-Verlag.

Zwieniecki MA, Holbrook NM. 2000. Bordered pit structure and vessel wall surface properties. implications for embolism repair. *Plant Physiology* **123**: 1015–1020.

Zwieniecki MA, Holbrook NM. 2009. Confronting Maxwell's demon: biophysics of xylem embolism repair. *Trends in Plant Science* **14**: 530–534.

Zwieniecki MA, Melcher PJ, Ahrens ET. 2013. Analysis of spatial and temporal dynamics of xylem refilling in *Acer rubrum* L. using magnetic resonance imaging. *Frontiers in Plant Science* **4**: 265.

Supporting Information

Additional supporting information may be found in the online version of this article.

Fig. S1 Transverse section from light microscopy shows the anatomy of tracheids close to the pith in *Sequoia sempervirens.*

Fig. S2 Transverse slices from microCT show the formation of embolism in tracheids of *Sequoia sempervirens.*

Movie S1 Movie produced from radial serial X-ray microCT sections showing embolized tracheids of a branch trace in the xylem of a *Sequoia sempervirens* sapling.

Please note: Wiley Blackwell are not responsible for the content or functionality of any supporting information supplied by the authors. Any queries (other than missing material) should be directed to the *New Phytologist* Central Office.